

# MAGNETIC ANOMALIES OVER PSRs NEAR THE LUNAR SOUTH POLE: IMPLICATIONS FOR SOLAR WIND ION FLUX MODELING. L. L. Hood, Lunar and Planetary Laboratory, University of Arizona, Tucson, Arizona, 85721, USA, lon@lpl.arizona.edu

**Introduction:** Solar wind ion sputtering is one of several non-negligible loss mechanisms for water ice in permanently shadowed regions (PSRs) near the lunar poles (e.g., [1]). Previous published model estimates of the solar wind ion flux onto the surfaces of lunar south polar craters have considered only the ambient solar wind flow and effects of topography [2]. We have recently reported mapping of magnetic anomalies at low altitudes in the lunar polar regions [3,4]. While anomalies are relatively weak over the area near the north pole, significant anomalies are present over the south polar region, including over several permanently shadowed craters. Here, further evidence for the existence of anomalies over PSRs is presented and the need for both improved mapping and improved modeling, taking into account deflection of solar wind ions by the observed crustal fields, is emphasized.

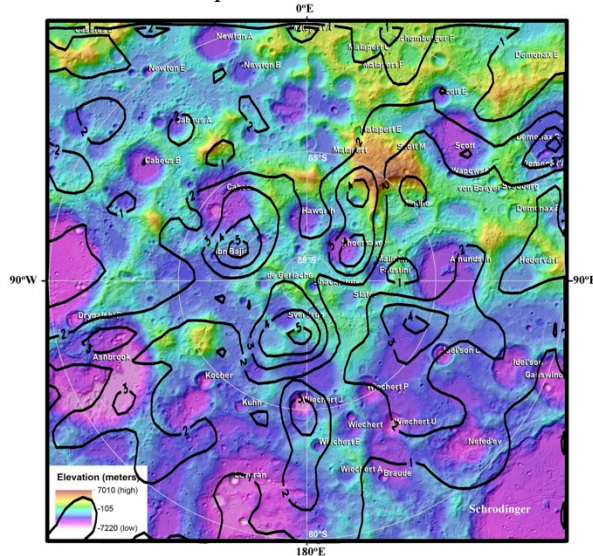


Figure 1

**Mapping:** The mapping method [5] consists of first constructing regional maps of improved accuracy over individual areas by selecting only the best magnetometer measurements (lowest altitude with least amount of external field contamination) over those specific areas. Once the best measurements are identified, an equivalent source dipole (ESD) technique (e.g., [6]) can be applied to normalize the measurements to a constant altitude. Individual regional maps can then be joined together to produce a larger-scale map. A large-scale map of the crustal field has recently been constructed using this approach at 30 km altitude covering latitudes from 65°S to 65°N [5]. Interpretation of the large-scale map

supports the hypothesis that many lunar magnetic anomaly sources consist of impact basin ejecta that is enriched in iron from the impactor.

Figure 1 shows a map of the field magnitude at 20 km altitude over the south polar region (~ 80°S to the pole) produced from Kaguya magnetometer data [7] using the above methodology. After two-dimensional filtering, the map has an effective horizontal resolution of ~ 51 km and is superposed onto a labeled topographic map [8] of the region. The contour interval is 1 nT. A series of moderately strong anomalies are in the near vicinity of the pole. One anomaly lies nearly over Shoemaker crater and another overlaps with Sverdrup crater.

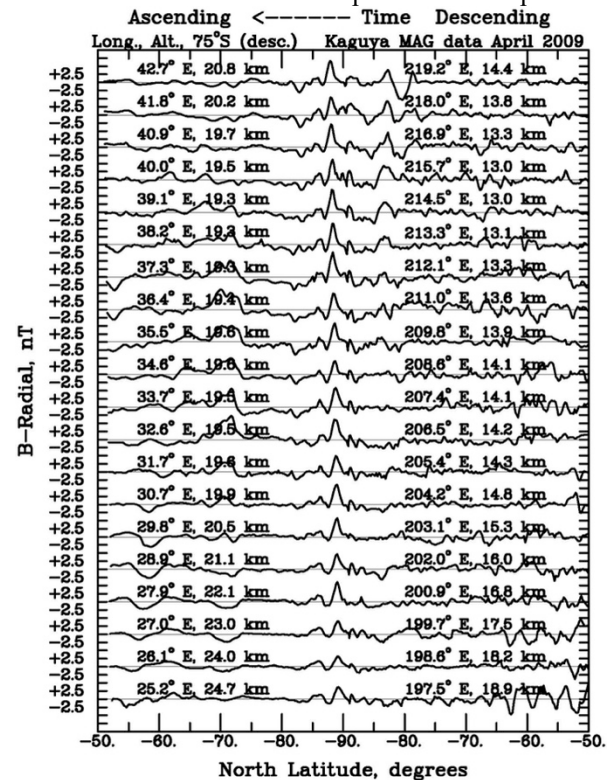


Figure 2

**Selected Orbit Passes:** In order to investigate further the existence of anomalies over these craters, direct radial field measurements along individual orbit tracks can be analyzed. Figure 2 plots radial field measurements from April of 2009 along a series of low-altitude Kaguya orbits that pass close to the south pole. Time along the orbits progresses from right to left; the descending part is therefore on the right of the center while the ascending part is on the left. Longitude and altitude at 75°S are given on both parts. Longitudes at 75°S on descending passes change rapidly near the pole and

become nearly 180° opposite at 75°S on ascending passes. An anomaly located close to the pole is prominent on these orbit passes. Its repetition on successive orbits confirms its lunar origin. It has an unfiltered amplitude approaching +7 nT for the ascending pass near 39°E at 75°S, for example.

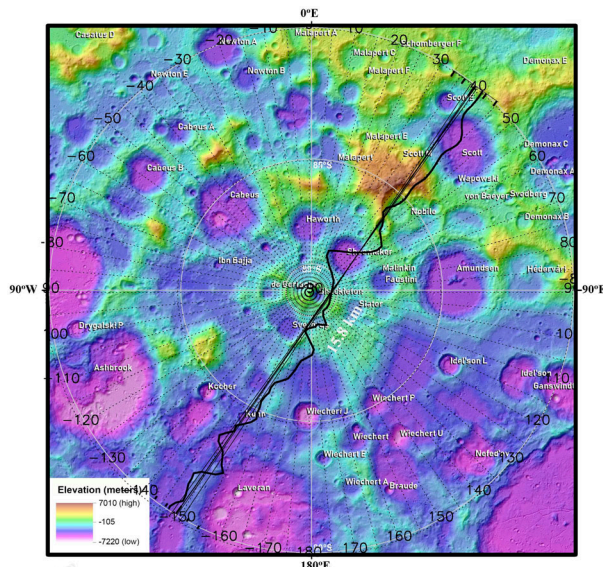


Figure 3

Figure 3 superposes several of these orbit tracks onto the topographic map of Stopar and Meyer [8]. The radial field amplitude along one of these passes (April 20, 2009; 14:49 UT; 36.4°E at 75°S on the ascending side) is plotted on the figure. The altitude ranges from ~ 14 km on the descending side at 80°S to ~ 18 km on the ascending side at 80°S. This track passes within 1° of the pole along the northern edge of Shackleton crater at an altitude of 15.8 km and continues through the interior of Shoemaker crater. The radial field anomaly overlaps the interior of Shoemaker while the field amplitude near Shackleton is small (< 1 nT).

**Discussion and Conclusions:** Based on evidence consistent with the iron-enriched ejecta mechanism for producing magnetic anomalies associated with young lunar basins [5], at least some of the polar anomalies mapped here may be related to the Schrödinger basin-forming impact. Schrödinger is the second youngest impact basin (i.e., crater with diameter > 300 km) on the Moon (e.g., [9]), with an absolute age of less than 3.9 Gyr. The anomalies centered on the south pole are located adjacent to Schrödinger and could have sources in the form of iron-enriched ejecta from this impact event.

It is important to note that some longitude sectors in Figures 1 and 3 were incompletely covered by high-quality, low-altitude KG passes. For this reason, two-dimensional filtering with an effective filter dimension of ~ 51 km (1.67° of latitude) was necessary. Future

orbital magnetometer measurements at low altitudes over the south polar region are therefore still much needed to fill in coverage gaps and allow construction of maps with better accuracy and higher horizontal resolution.

Considering the low angle of solar wind incidence relative to the horizontal near the lunar poles, the south polar anomalies of Figure 1 should be effective in shielding the underlying terrain from much of the solar wind ion bombardment. The south polar anomalies have peak amplitudes of about one-quarter that of the Reiner Gamma anomaly at a common altitude. The Reiner Gamma anomaly significantly deflects the solar wind ion bombardment, which is a major part of the explanation for its correlated higher-albedo swirl markings (e.g., [10]). The angle of solar wind incidence at Reiner Gamma ranges from nearly grazing to nearly vertical depending on the time of the lunar day. The angle of solar wind incidence at the lunar south pole is always nearly grazing. Simplified ion trajectory calculations considering only the Lorentz force show that protons with velocities near 400 km/sec (typical of the solar wind) are deflected much more strongly and shield a larger surface area at incidence angles of 40° or more from the vertical (ref. 11; their Fig. 12). Anomalies near the lunar south pole are therefore likely capable of shielding large areas in their vicinities from most or all of the ion bombardment. Future simulations using state-of-the-art plasma physics models are needed to quantify this further.

**Acknowledgments:** Supported under a grant from the NASA LDAP program (80NSSC21K1478). Kaguya (SELENE) vector magnetometer data are available from the Japan Aerospace Exploration Agency at <http://darts.isas.jaxa.jp/planet/pdap/selene>.

**References:** [1] Zimmerman, M. I. et al. (2011) *GRL*, 38, No. 2548. [2] Rhodes, D. J. & W. M. Farrell (2020), *Planet. Sci. J.*, 1:13 (8 pp), doi:10.3847/PSJ/ab8939 [3] Hood, L. L. et al. (2022) 53<sup>rd</sup> LPSC, abstract # 2102. [4] Hood, L. L. et al. (2022) *GRL*, in review. [5] Hood L. L. et al. (2021) *JGR Planets*, 126, doi: 10.1029/2020JE006667. [6] Hood, L. L. (2015) *GRL*, 42, 10,565-10,572, doi:10.1002/2015GL066451 [7] Tsunakawa, H. et al. (2010) *Space Science Reviews*, 154, 219-251. [8] Stopar, J. & H. Meyer (2019), *Topographic Map of the Moon's South Pole (80°S to Pole)*, LPI Contribution 2169, <https://repository.hou.usra.edu/handle/20.500.11753/1254>. [9] Wilhelms, D. E. (1984) In M. Carr (Ed.), *The geology of the terrestrial planets* (pp. 107-205). NASA [10] Kramer, G. Y. et al. (2011) *J. Geophys. Res. Planets*, 116, E00G18, doi:10.1029/2010JE003729. [11] Hood, L. L. & C. Williams (1989), *Proc. Lunar Planet. Sci. Conf. 19<sup>th</sup>*, 99-113.